J. Phys. D: Appl. Phys. **44** (2011) 325402 (5pp) doi:10.1088/0022-3727/44/32/325402

Manipulation of palladium nanoparticles in a 20 nm gap between electrodes for hydrogen sensor application

Binh Le Huy[1], Sanjeev Kumar[2] and Gil-Ho Kim[1]

[1] Department of Electronic and Electrical Engineering and Sungkyunkwan Advanced Institute of Nanotechnology, Sungkyunkwan University, Suwon 440-746, Korea
[2] London Centre for Nanotechnology, University College London, 17-19 Gordon Street, London WC1H0AH, UK

E-mail: ghkim@skku.edu

Received 6 April 2011, in final form 7 June 2011
Published 25 July 2011
Online at stacks.iop.org/JPhysD/44/325402

Abstract
This study reports a promising, cost-effective nanoscale hydrogen sensor fabricated using the dielectrophoresis (DEP) process. Palladium nanoparticles (NPs) of diameter in the range 2–4 nm were assembled in a 20 nm gap between electrodes under optimized DEP parameters of frequency, voltage and assembling time of 1 M Hz, 1.5 V and 90 s, respectively. The fabricated nanoscale device was powered by applying a dc voltage of 10 mV across nanogap electrodes and temporal change in resistance at an operating temperature of 160 °C was recorded in the presence of 3000 ppm of hydrogen gas. A rise and recovery times of 100 s and 300 s, respectively, in the temporal hydrogen gas response characteristic were observed which could be attributed to the hydride formation due to the strong affinity of assembled palladium NPs towards hydrogen. The nanoscale device was sensitive enough to respond to hydrogen presence even at 30 °C. Preliminary results show the potential of DEP in fabricating cost-effective nanoscale hydrogen sensor.

(Some figures in this article are in colour only in the electronic version)

1. Introduction

Nanoparticles (NPs) are currently of intense research interest due to their wide variety of potential applications in various fields such as biology, medicine, optics, sensors and electronics [1–3]. In the field of hydrogen (H_2) sensing, various kinds of NPs have been investigated; however, palladium (Pd) NP has gained considerable attention due to its remarkable chemical reactivity with hydrogen and thus is one of the most sought after materials for hydrogen sensing [4]. Pd has been investigated extensively as a selective catalytic material for absorption and desorption of hydrogen due to its large sticking coefficient and a very strong affinity towards hydrogen absorption which is speculated to be more in nanoscale range because of increased specific surface area [4–6]. The catalytic behaviour of Pd has been extensively studied in bulk, thin and thick films, clusters, nanowires and nanoparticulate thin films [5–9]. In these studies, a variation in conductivity due to Pd hydride (PdH_x) formation has been observed, which is attributed to be the primary mechanism for hydrogen sensing. Interestingly, there are mixed reports on variation in conductivity of nanostructures of Pd such as nanowires and nanoparticulate thin films. While the former shows an increase in conductivity, the latter exhibits a decrease in conductivity on hydrogen exposure [4, 5, 10, 11]. Observations of such mixed behaviour in conductivity encourage further studies on the hydrogen sensing characteristics of Pd nanostructures. Even though different kinds of nanostructures of Pd have been tried for hydrogen sensing purposes, but there is scarcely any literature report on the hydrogen sensing characteristics of a nanoscale device consisting of a few Pd NPs. This could be due to the fact that fabrication of nanoscale devices consisting of a few NPs poses great challenges, especially when NPs are just a few nanometres in size. Assembling NPs between a pair of electrodes could either be done by established, expensive fabrication technique such as e-beam lithography

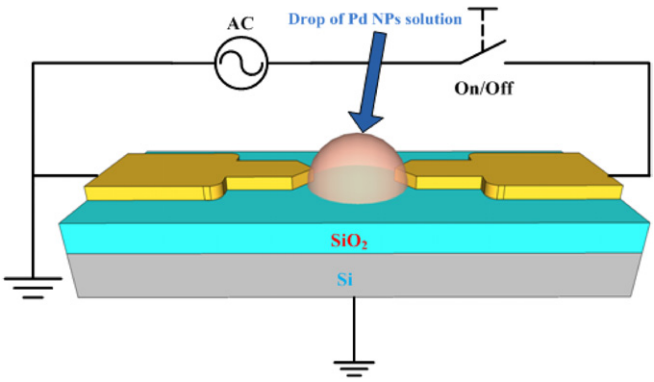

Figure 1. Schematic diagram of the experimental setup used for the DEP process.

or efficient, cost-effective process such as dielectrophoresis (DEP), which has recently gained tremendous interest due to its simplicity and high yield in assembling materials such as gold (Au) nanocolloids, carbon nanotubes, microorganism, DNA and nanowires, between electrode gaps for various potential nanoscale device applications [12–22].

Motivated by the fact that DEP could significantly simplify the fabrication of nanoscale hydrogen sensor, a study on assembling Pd NPs between a pair of Au electrodes spaced 20 nm apart was performed and the assembling process as well as the preliminary H_2 sensing characteristics of such a device are presented in this paper.

2. Experimental details

The Pd NPs used in this work (purchased from Strem Chemicals Inc.) have a diameter in the range 2–4 nm. The Au nanogap electrodes were fabricated on the oxide-coated silicon substrate using standard e-beam lithography, metal evaporation and lift-off techniques [20, 21] . Each chip consists of ten pairs of electrodes with a gap of 20 nm in between each pair (figure 1, [20]). Before performing the DEP process, chips were cleaned using oxygen plasma for 10 min at an oxygen flow-rate of 30 sccm, then rinsed in ethanol for 5 s, and blown dry using nitrogen gas. The experimental setup used for the ac DEP process is shown in figure 1. An approximately 1 μl drop of aqueous Pd NPs solution was placed in the centre of the cleaned chip using a micropipette and an ac signal was applied across the electrodes to begin the DEP process. After the DEP process, scanning electron microscopy (SEM) was used to examine the dielectrophoretic alignment of Pd NPs into the nanogap electrodes. The composition of the sample was examined by energy-dispersive x-ray spectroscopy (EDX). Current–voltage (I–V) characteristics of the fabricated nanoscale device were studied using Keithley I–V measurement system (Model 4200 FCS).

The hydrogen sensing characteristics of the Pd NPs-based nanoscale device were studied using an indigenously designed H_2 sensing test chamber assembly. The test chamber assembly consists of a mixing chamber connected to the main chamber (capacity ~5 L) via an inlet valve. The main chamber consists of an *in situ* heating arrangement with a maximum allowable temperature of 160 °C with an accuracy of ±0.1 °C min^{-1}. The mixing chamber, on the other hand, has two input valves, one corresponding to H_2 gas and other for carrier gas (a mixture of N_2 and O_2 gases). Mass-flow controllers are connected across the input terminals of the mixing chamber to control the flow of gases. The gases are withdrawn from the main chamber by opening the outlet value which was connected through a baffle valve to an oil-sealed rotary pump. During the experiments, a pressure of 5 mTorr was first created in the main chamber and then the temperature was controlled at the desired value at a slow ramping rate of 10 °C min^{-1}. Temporal H_2 sensing characteristics were performed by applying a dc bias of 10 mV across the fabricated Pd-based nanoscale device.

3. Results and discussion

3.1. Pd Nanoscale device fabrication

Basically, assembling NPs using ac DEP depends on frequency (f) of the applied ac signal, peak-to-peak voltage (V_{pp}) and the duration (t) of the DEP process [14, 20]. It is important to optimize the DEP parameters to increase the yield of successful assembly. We performed our experiments under optimized f of 1 MHz, V_{pp} of 1.5 V and t of 90 s. The yield of successful assembly under the optimized parameters was almost 90%. A detailed study on optimized assembly of Pd NPs in a 20 nm gap between electrodes would be published elsewhere. The NPs would assemble in the electrodes gap when they experience positive DEP force. The time-averaged DEP force (F_{DEP}) is given by $F_{DEP} = 2\pi\varepsilon_m R^3 \mathrm{Re}[K(\omega)]\nabla E_{rms}^2$, where ε_m is the permittivity of the aqueous medium, R is the radius of the NP, $\underline{K}(\omega)$ is the Clausius–Mossotti factor and E_{rms} is the rms value of the electric field. The nature of F_{DEP} is primarily decided by $\underline{K}(\omega)$. In the complex form, $\underline{K}(\omega)$ is defined as [22]

$$K(\omega) = \frac{\varepsilon_p - \varepsilon_m - (j/\omega)(\sigma_p - \sigma_m)}{\varepsilon_p + 2\varepsilon_m - (j/\omega)(\sigma_p + 2\sigma_m)}, \quad (1)$$

where ε_p and ε_m are the permittivities of the NPs and aqueous medium, σ_p and σ_m are the conductivities of the NPs and medium, j is $\sqrt{(-1)}$, and ω is the angular frequency of the ac voltage. Expanding and factorizing yielded the real part of $\underline{K}(\omega)$ as

$$\mathrm{Re}[K(\omega)] = \frac{(\varepsilon_p - \varepsilon_m)(\varepsilon_p + 2\varepsilon_m) + (1/\omega^2)(\sigma_p - \sigma_m)(\sigma_p + 2\sigma_m)}{(\varepsilon_p + 2\varepsilon_m)^2 + (1/\omega^2)(\sigma_p + 2\sigma_m)^2}. \quad (2)$$

F_{DEP} can be positive or negative depending on the permittivities and conductivities of the NPs and the aqueous medium, respectively, and the frequency of the ac signal (equations (1) and (2)). Positive values of Re[$\underline{K}(\omega)$] lead to a positive time-averaged DEP force pulling NPs towards the strong electric field regions, whereas negative values of Re[$\underline{K}(\omega)$] lead to a negative time-averaged DEP force that repels NPs from the strong electric field regions. Based on equation (2) and the conductivities and permittivities of Pd NPs [i.e. $\sigma_p = 9.5\times10^{10}$ μS cm^{-1} and $\varepsilon_p = 6.25\varepsilon_0$ F m^{-1} ([23])] and de-ionized water

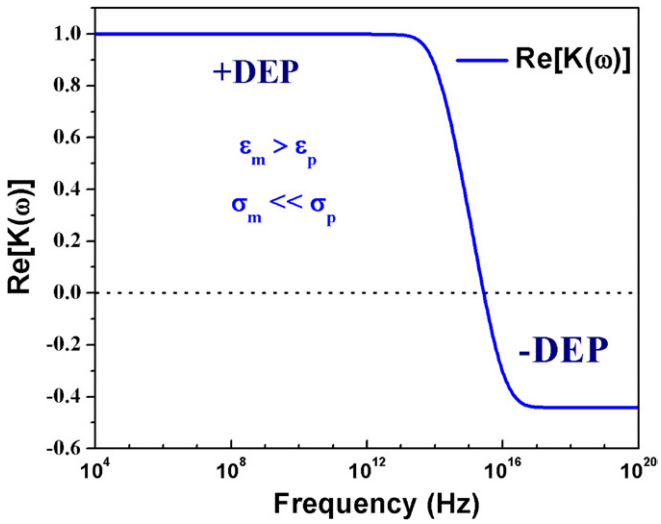

Figure 2. Variation in real part of Clausius–Mossotti factor, Re[$\underline{K}(\omega)$] with frequency.

(i.e. $\sigma_m = 1.0\,\mu S\,cm^{-1}$ and $\varepsilon_m = 78\varepsilon_0\,F\,m^{-1}$ ([22])), the real part of Re[$\underline{K}(\omega)$] as a function of the frequency is plotted and shown in figure 2. It may be noted that the optimized frequency value of 1 MHz used in the present work lies towards positive DEP, and is therefore in agreement with the observed behaviour.

Figure 3(*a*) shows the assembly of Pd NPs between electrodes gap of 20 nm. The inset shows a magnified view of the Pd nanobridge where Pd NPs could be seen in almost molten state. It may be noted that some NPs are seen on the surface of the electrodes in addition to their presence in the electrodes gap which could be due to various other factors associated with DEP. DEP is a complicated process and does depend on lots of parameters including applied ac voltage, frequency, time, temperature, humidity, etc. During the DEP process, a non-zero DEP force is exerted on the Pd NPs and the motion of the NPs changes from random due to Brownian motion to the directional motion towards the highest voltage zone (between the electrode tips) in order to form Pd nanobridge. It is important to note that the gap between the electrodes is 20 nm and the NPs' diameter ranges between 2 and 4 nm. It has been experimentally observed that the trapping time has a significant role on the manipulation of NPs into the nanogap electrodes. The larger the trapping time, the more the possibility of NPs to be captured between the electrodes gap [20]. In addition, there are some other factors like V_{pp} and f which play a vital role in assembling NPs. It is practically difficult to realize a unique trapping parameter which could allow assembling all the NPs into the electrodes gap due to the dependence of DEP parameters on a number of associated factors such as size dependent permittivity and conductivity, electrode polarization, thermal effects and ac acousto-osmosis effects [24]. It may further be noted that Pd NPs are not of a fixed diameter so they experience a range of DEP force, and hence influence the assembly of NPs. All these combined factors could be attributed to the appearance of some NPs on the surface of the electrodes. The NPs on the surface of electrodes are too small in number and size that they would hardly have any influence on the hydrogen sensing characteristics being observed due to the nanobridge.

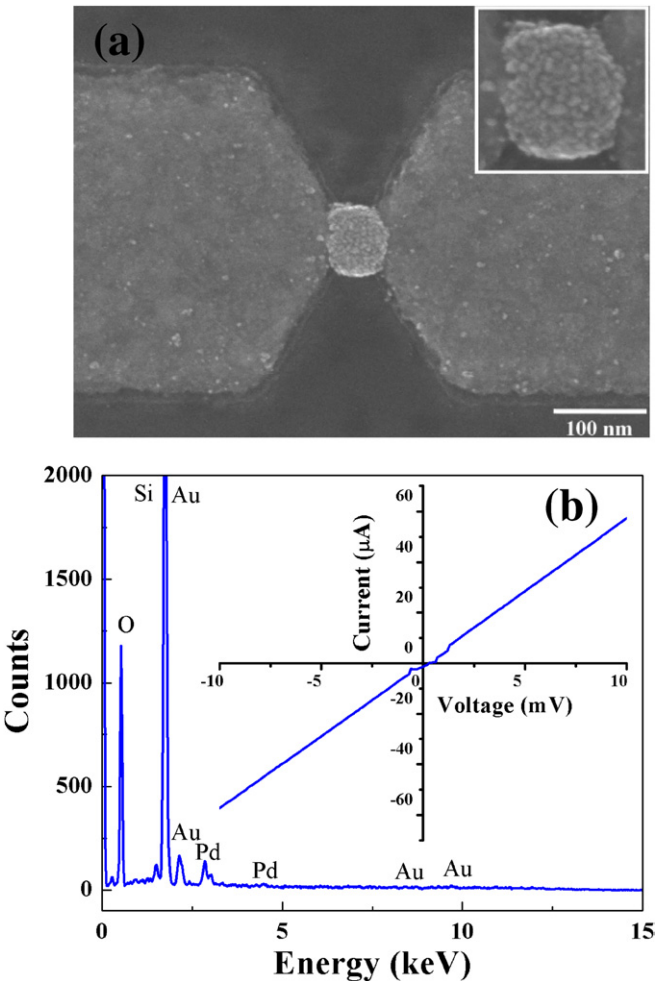

Figure 3. (*a*) SEM image of the Pd NPs assembled between a 20 nm gap electrodes. Inset: close-up view of the Pd nanobridge. (*b*) EDX spectrum of fabricated Pd NPs-based nanoscale device. Inset: I–V characteristic of the Pd NPs-based nanoscale device.

EDX spectrum shown in figure 3(*b*) revealed various peaks such as (a) Pd emanating from NPs bridging the Au electrodes, (b) silicon and oxygen emanating from the silicon-dioxide/Si substrate and (c) Au emanating from the Au electrodes. I–V measurements were performed on the fabricated Pd-based nanoscale device and one such characteristic is shown in the inset of figure 3(*b*). It is important to note that the nanoscale device exhibits a linear I–V characteristic indicating ohmic contacts between the Pd nanobridge and Au electrodes. The ohmic nature of the measured current–voltage (I–V) curve shows that a continuous nanobridge was formed across the gap between the electrodes as a result of localized melting [15].

3.2. Hydrogen sensing response characteristics

The fabricated Pd NPs-based nanoscale device was loaded into the test chamber assembly to study the hydrogen sensing characteristics. Figure 4 shows the temporal hydrogen response characteristics of the Pd-based nanoscale device at two different hydrogen concentrations of 5% and 100%

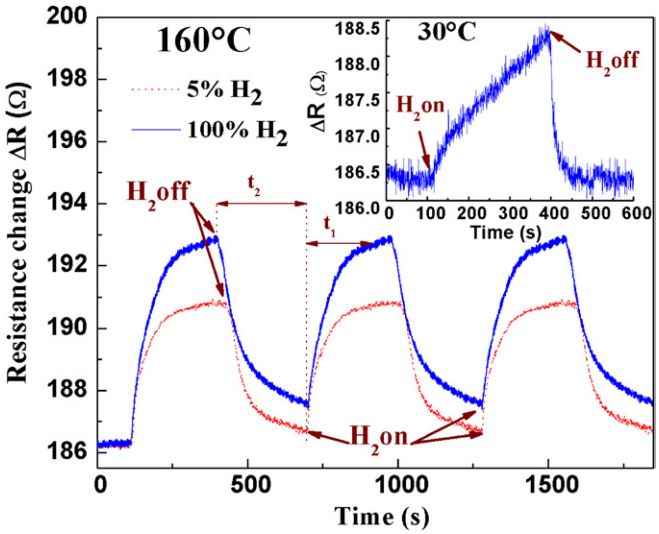

Figure 4. Temporal changes in resistance of the Pd NPs-based nanoscale hydrogen sensor when subjected to cyclic H_2 loading and unloading at an operating temperature of 160 °C, and at different H_2 concentrations of 5% and 100%; t_1, t_2 indicates rise and recovery times, respectively. Inset: Temporal change in resistance of the nanoscale device at 30 °C.

(3000 ppm) at an operating temperature of 160 °C. When the hydrogen gas was loaded into the main chamber a quick rise in resistance followed by a gradual rise was observed. On removal of hydrogen gas from the main chamber when the change in resistance was tending to saturate, a sudden decrease in resistance was observed. Similar to rise trend, the decrease in resistance had two components, first a quick decrease and then a gradual decrease. On comparing the rise and recovery components in the temporal response characteristic, it was found that the sensor had a rise and recovery time of 100 s and 300 s, represented by t_1 and t_2, respectively in the temporal response curve shown in figure 4.

Figure 5 shows the mechanism of H_2 sensing in Pd NPs-based nanoscale device. When H_2 gas is introduced in the test chamber, adsorption of H_2 on Pd nanobridge takes places (figure 5(*a*)). The adsorbed H_2 molecules dissociate on the surface of Pd NPs. At an operating temperature of 160 °C, the hydrogen atoms gain sufficient kinetic energy and diffuse into the lattice of Pd to form Pd hydrides (PdH_x) (figure 5(*b*)). The expansion of PdH_x lattice results in an increase in resistance of the Pd nanobridge (figure 4) [5]. On removal of H_2 from the main chamber by opening the outlet valve, a sudden drop in H_2 concentration occurs and the hydrogen, which participated in forming PdH_x, escapes from the Pd nanobridge and results in a decrease in resistance. Figure 5(*c*) shows desorption of hydrogen from the lattice of PdH_x.

Other groups have also performed H_2 sensing characteristics of nanostructures of Pd. Jeon *et al* [25] reported the hydrogen sensing response characteristics of Pd nanowires having electrodes patterned with e-beam lithography in the concentration range 200–20 000 ppm. With an increase in hydrogen concentration, the response time was steadily found to increase from 22 to 600 s corresponding to hydrogen concentration of 200 and 20 000 ppm, respectively. Joshi *et al* [5] recently reported a Pd thin film-based H_2 sensor able to detect small

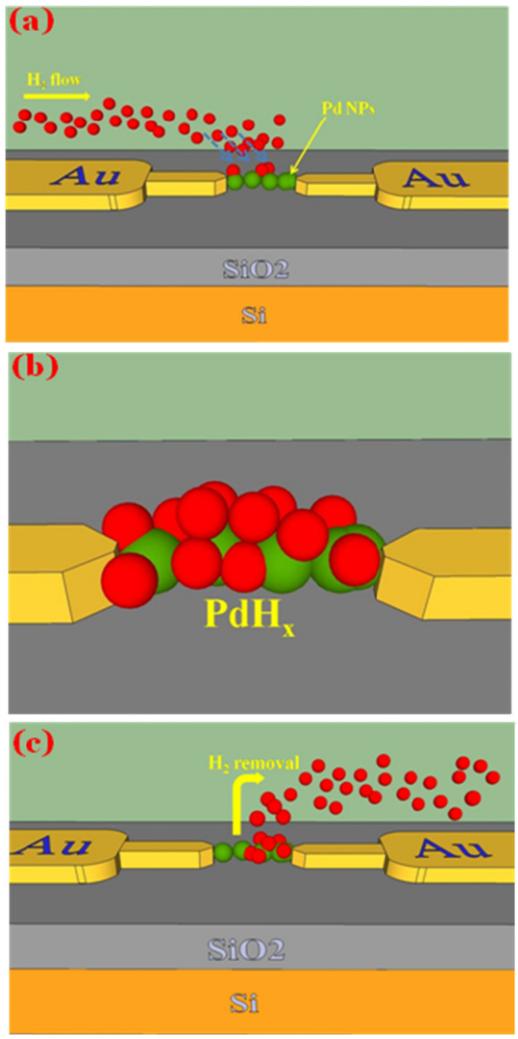

Figure 5. Mechanism of H_2 absorption and desorption across the Pd nanobridge formed between a pair of electrodes: (*a*) adsorption of hydrogen across the Pd nanobridge when hydrogen was loaded into the measurement chamber, (*b*) PdH_x formation across the Pd nanobridge and (*c*) desorption of hydrogen on removal of gases from the measurement chamber.

H_2 concentration of 1.0% exhibiting a larger change in resistance of ~400 Ω with longer rise and recovery times of 1000 s and 2000 s, respectively. These sensors are responsive to hydrogen exposure, however, accompanied by large response time. In addition, these sensors require a complicated fabrication process, which adds to the cost of the sensors and most importantly devices are not small enough for integration into nanoscale electronic chip. On the other hand, the nanoscale device reported in this work proposes a compact, efficient and cost-effective nanoscale hydrogen sensor fabricated using the DEP process. The size of the chip is 3.5 mm × 3.5 mm and a very low bias of 10 mV is required to power the device.

It may also be noted that a change in resistance of ~7 Ω was observed for a hydrogen gas concentration of 100% in comparison with hydrogen concentration of 5% where the change in resistance was ~ 4.5 Ω. Even though the sensor shows good temporal response characteristics and the responsivity is very appreciable, the change in resistance

observed in this work is not very significant, which could be due to the short length of the Pd nanobridge (20 nm). We have not been able to figure out the actual reason for a small change in resistance; however, this may be attributed to the physical nature of the nanobridge. Figure 3(*a*) indicates that Pd NPs are almost in completely molten state which could have a substantial effect in deciding the response time of the sensor. A continuous nanobridge with almost all the constituents Pd NPs in the molten state could be understood as a bulk system rather than a nanobridge where the constituent NPs maintain their original shape without being melted. The latter system could have more reactivity with hydrogen due to increased surface-to-volume ratio than the former one. Efforts are continued in controlling the melting of the NPs after they bridge the nanogap electrodes to investigate the influence of two geometries on the response time and sensitivity of the device.

To test the potential of Pd-based nanoscale hydrogen sensor at around room temperature, hydrogen sensing was measured at an operating temperature of 30 °C and the result is shown in the inset of figure 4. It may be observed that the initial response of the Pd NPs-based nanoscale sensor was fairly quick when hydrogen atoms dissociate on the surface of the Pd nanobridge and incorporate into the Pd lattice [4]. Due to lower diffusion rate of hydrogen into the Pd nanobridge at lower temperature, the resistance change in the Pd nanobridge was slow but the device was fairly responsive to hydrogen presence. Such elementary results show the potential of DEP in realizing low-temperature Pd-based nanoscale hydrogen sensor.

4. Conclusion

Hydrogen sensing response in Pd NPs dielectrophoretically assembled between a pair of electrodes was performed. Results suggest a simple and efficient method to fabricate Pd NPs-based H_2 sensor with a possibility of room temperature operation.

Acknowledgment

This research was supported by the National Research Foundation of Korea (NRF) funded by the Ministry of Education, Science and Technology (Grant No R32-2008-000-10204-0 and KRF-2008-314-D00251).

References

[1] Salta O V 2004 *J. Nanobiotechnol.* **2** 3
[2] Bezryadin A, Dekker C and Schmid G 1997 *Appl. Phys. Lett.* **71** 1273–5
[3] Khondaker S I, Luo K and Yao Z 2010 *Nanotechnology* **21** 095204
[4] Khanuja M, Varandani D and Mehta B R 2007 *Appl. Phys. Lett.* **91** 253121
[5] Joshi R K, Krishnan S, Yoshimura M and Kumar A 2009 *Nanoscale. Res. Lett.* **4** 1191–6
[6] Lewis F A 1967 *The Palladium–Hydrogen System* (London: Academic)
[7] Dankert O and Pundt A 2002 *Appl. Phys. Lett.* **81** 1618–20
[8] Pundt A, Suleiman M, Bahtz C, Reetz M T, Kirchheim R and Jisrawi N M 2004 *Mater. Sci. Eng.* B **108** 19–23
[9] Ferrara V L, Alfano B, Massera E and Francia G D 2008 *IEEE Trans. Nanotechnol.* **7** 776–81
[10] Kobayashi H, Yamauchi M, Kitagawa H, Kubota Y, Kato K and Takata M 2008 *J. Am. Chem. Soc.* **130** 1828–9
[11] Xu T, Zach M P, Xiao Z L, Rosenmann D, Welp U, Kwok W K and Crabtree G W 2005 *Appl. Phys. Lett.* **86** 203104
[12] Pohl H A 1978 *Dielectrophoresis: The Behavior of Neutral Matter in Nonuniform Electric Fields* (Cambridge: Cambridge)
[13] Hughes M P 2000 *Nanotechnology* **11** 124–32
[14] Jones T B 1995 *Electromechanics of Particles* (Cambridge: Cambridge University Press)
[15] Barsotti R J, Jr , Vahey M D, Wartena R, Chiang Y M, Voldman J and Stellacci F 2007 *Small* **3** 488–99
[16] Cicoria R and Sun Y 2008 *Nanotechnology* **19** 485303
[17] Asbury C L, Diercks A H and Engh G V D 2002 *Electrophoresis* **23** 2658–66
[18] Boote J J and Evans S D 2005 *Nanotechnology* **16** 1500–5
[19] Wosik J, Padmaraj D, Darne C and Zagozdozon-Wosik W 2006 *ISSO Annual Report* (http://www.isso.uh.edu/publications/A2006/2006_108_wosik.pdf), 108–10
[20] Yoon S H, Kumar S, Kim G-H, Choi Y S, Kim T W and Khondaker S I 2008 *J. Nanosci. Nanotechnol.* **8** 3427–33
[21] Kumar S, Yoon S H and Kim G-H 2009 *Curr. Appl. Phys.* **9** 101–3
[22] Gierhart B C, Howitt D G, Chen S J, Smith R L and Collins S D 2007 *Langmuir* **23** 12450–6
[23] Cioffi N, Ceglia D de, De Sario M, D'Orazio A, Petruzzelli V, Prudenzano F, Scalora M, Trevisi S and Vincenti M A, http://arxiv.org/abs/physics/0701233v1
[24] Kumar S, Seo Y-H and Kim G-H 2009 *Appl. Phys. Lett.* **94** 153104
[25] Jeon K J, Lee J M, Lee E and Lee W 2009 *Nanotechnology* **20** 135502